LOW-COMPLEXITY EQUALIZATION OF TIME-VARYING CHANNELS IN A SINGLE-CARRIER SYSTEM

Zijian Tang and Geert Leus

Delft University of Technology - Fac. EEMCS
Mekelweg 4, 2628 CD Delft, The Netherlands
{z.tang, g.leus}@tudelft.nl

ABSTRACT

We consider a single-carrier transceiver, which abides with both fast channel fading and severe inter-block interference. To enable a low-complexity frequency-domain equalizer, it is desired that 1) the channel matrix be approximately banded; and 2) the inter-block interference be reduced. In this paper, we propose an extended data model, which incorporates a receiver window to enforce these two conditions.

keywords: single-carrier, BEM, time-varying channels, IBI.

1. INTRODUCTION

In a single-carrier transmission system over a lengthy channel, it is more efficient to carry out the equalization in the frequency domain. However, when neither the inter-block interference (IBI) can be totally eliminated nor the channel's time-variation within a single block can be ignored, the resulting frequency-domain (FD) channel matrix is not diagonal but full. This implies that the simple one-tap equalizer [1], which is successfully applied to IBI-free time-invariant systems, is not viable any more. To equalize such a full-matrix channel is expensive. Therefore, many low-complexity equalizers rely on the assumption that the FD channel matrix is approximately banded [2, 3, 4]. To enhance the equalization precision, we need to reduce the band approximation error as well as the impact of the IBI while still maintaining the same low complexity. This can be achieved, e.g., by using a receiver window as shown in [2, 3, 4].

In this paper, we will propose two new windowing techniques. The first will be based on the original data model (ODM), which describes the actual input/output (I/O) relationship. Neglecting the out-of-band interference, we can show that the resulting windowed FD channel can be related in the time domain to a special basis expansion model (BEM)[5], referred to as the critically-sampled complex exponential BEM ((C)CE-BEM) [6]. Actually, such a link also exists in [2], but it is not straightforward to

observe. The second windowing technique will be based on the so-called extended data model (EDM), which still utilizes the ODM, but extends it to a larger scale. This time, the resulting windowed FD channel can be related in the time domain to an oversampled complex exponential BEM ((O)CE-BEM) [7]. The connection between these two windows with the (C)CE-BEM and (O)CE-BEM, respectively, will be explored in our window design. Since the (C)CE-BEM and (O)CE-BEM generally render different modeling performances as shown in [8], the resulting receivers will also exhibit unique behaviors, which eventually have an impact on the equalization performance.

Notation: We use upper (lower) bold face letters to denote matrices (column vectors). $(\cdot)^*$, $(\cdot)^T$ and $(\cdot)^H$ represent conjugate, transpose and complex conjugate transpose (Hermitian), respectively. $\mathcal{E}\{\cdot\}$ stands for the expected value. $\odot$ represents the Schur-Hadamard (element-wise) product. We use $[\mathbf{x}]_p$ to indicate the $(p+1)$st element of $\mathbf{x}$, and $[\mathbf{X}]_{p,q}$ to indicate the $(p+1, q+1)$st entry of $\mathbf{X}$. Further, we let $\mathbf{I}_N$ denote an $N \times N$ identity matrix, $\mathbf{0}_{M \times N}$ an $M \times N$ all-zero matrix, and $\mathbf{1}_{M \times N}$ an $M \times N$ all-one matrix. $\mathbf{e}_k$ stands for a unit vector with a one at the $(k+1)$st position. $\mathbf{F}_N$ denotes the unitary N-point DFT matrix with $[\mathbf{F}_N]_{p,q} = \frac{1}{\sqrt{N}}e^{-j\frac{2\pi}{N}pq}$.

2. DATA MODEL

Let us consider a communication system, where the channel is assumed to be a finite impulse response (FIR) filter with order L, i.e., if we use $h_{p,l}$ to denote the lth channel tap at the pth time-instance then $h_{p,l} = 0$ if $l < 0$ or $l > L$. Conform the FIR assumption, we can express the I/O relationship as

$$y_p = w_p \sum_{l=0}^{L} h_{p,l} s_{p-l} + v_p, \tag{1}$$

where w_p stands for the pth element of the window that is deployed at the receiver; y_p and v_p denote the observation sample and noise after windowing at the pth time-instance, respectively; and s_p the pth data symbol.
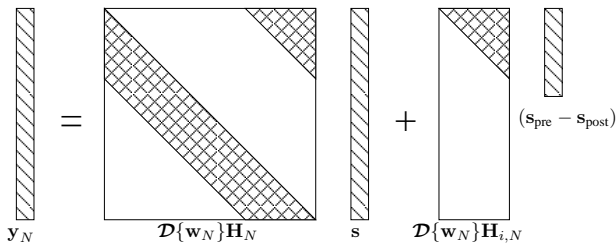
Figure 1: *The noiseless original data model.*

This paper deals with time-varying channels, which implies that $h_{p,l} \neq h_{q,l}$ if $p \neq q$. The channel can be characterized by a statistical model. For instance, assuming a wide-sense stationary uncorrelated scattering (WSSUS) channel, we have

$$\mathcal{E}\{h_{p,l}h^*_{p-m,l-n}\} = \sigma_l^2 \gamma_m \delta_n. \qquad (2)$$

Here, δ_n denotes the Kronecker delta, σ_l^2 the variance of the lth channel tap, and γ_m the normalized time correlation.

For the remainder of the paper, we assume these statistics are perfectly known. Further, we assume the data symbols are zero-mean white with unit variance, i.e., $\mathcal{E}\{s_p s^*_{p-m}\} = \delta_m$, and the noise prior to windowing is zero-mean white with variance σ^2. Taking the window into account, this implies $\mathcal{E}\{v_p v^*_{p-m}\} = \sigma^2 \delta_m w_p w^*_{p-m}$.

3. FD EQUALIZATION BASED ON THE ODM

3.1. Equalization Scheme

Suppose that we are interested in the $N - L$ data symbols $[s_0, \cdots, s_{N-L-1}]^T$, whose information is present in the observation samples $\mathbf{y}_N := [y_0, \cdots, y_{N-1}]$. The I/O relationship in (1) can be expressed in a block form as

$$\mathbf{y}_N = \mathcal{D}\{\mathbf{w}_N\}\mathbf{H}_N\mathbf{s} + \boldsymbol{\epsilon}_N + \mathbf{v}_N, \qquad (3)$$

where $\mathbf{w}_N := [w_0, \cdots, w_{N-1}]^T$, $\mathbf{s} := [s_0, \cdots, s_{N-1}]^T$, and $\mathbf{v}_N := [v_0, \cdots, v_{N-1}]^T$. $\mathbf{H}_N$ stands for an $N \times N$ channel matrix with entries $[\mathbf{H}_N]_{p,n} := h_{p,\mathrm{mod}(p-n,N)}$. $\boldsymbol{\epsilon}_N := \mathcal{D}\{\mathbf{w}_N\}\mathbf{H}_{i,N}(\mathbf{s}_{\mathrm{pre}} - \mathbf{s}_{\mathrm{post}})$, where $\mathbf{H}_{i,N}$ is an $N \times L$ matrix with entries $[\mathbf{H}_{i,N}]_{p,n} := h_{p,p-n+L}$; $\mathbf{s}_{\mathrm{pre}}$ is a vector containing the data symbols from the previous block $\mathbf{s}_{\mathrm{pre}} := [s_{-L}, \cdots, s_{-1}]^T$; and $\mathbf{s}_{\mathrm{post}}$ is a vector containing the last L data symbols $\mathbf{s}_{\mathrm{post}} := [s_{N-L}, \cdots, s_{N-1}]^T$. The above I/O relationship in the noiseless case is illustrated in Fig.1.

Transformed into the frequency domain, (3) becomes

$$\mathbf{y}_{f,N} = \mathbf{H}_{f,N}\mathbf{F}_N\mathbf{s} + \boldsymbol{\epsilon}_{f,N} + \mathbf{v}_{f,N}, \qquad (4)$$

where $\mathbf{y}_{f,N}$ denotes the observation samples in the frequency domain $\mathbf{y}_{f,N} := \mathbf{F}_N\mathbf{y}_N$, and $\boldsymbol{\epsilon}_{f,N}$ and $\mathbf{v}_{f,N}$ are

similarly defined as $\mathbf{y}_{f,N}$. $\mathbf{H}_{f,N} := \mathbf{F}_N\mathcal{D}\{\mathbf{w}_N\}\mathbf{H}_N\mathbf{F}_N^H$ stands for the FD channel matrix. In the ODM scheme, the size of the DFT equals the number of observation samples. This will be in contrast with the EDM scheme of the next section, where the size of the DFT is larger than the number of observation samples.

The nuisance term $\boldsymbol{\epsilon}_{f,N}$ is caused by the IBI, and will not disappear even at a high signal to noise ratio (SNR). The IBI can be mitigated by the utility of a guard interval of length L_z, e.g., a cyclic-prefix (CP), a zero-prefix (ZP)[9] or a non-zero prefix (NZP) [10]. In the CP case,

$$[s_{-L_z}, \cdots, s_{-1}] = [s_{N-L_z}, \cdots, s_{N-1}], \qquad (5)$$

while in the ZP and NZP case,

$$[s_{-L_z}, \cdots, s_{-1}]^T = [s_{N-L_z}, \cdots, s_{N-1}]^T = \mathbf{p}, \qquad (6)$$

with $\mathbf{p}$ being a zero or non-zero pilot vector, respectively. For $L_z \geq L$, the IBI can be completely suppressed. In this paper, we will focus on the scenario where L_z assumes an arbitrary value.

Aside from the IBI and noise, the non-zero off-diagonal elements of $\mathbf{H}_{f,N}$ prevent the viability of a one-tap equalizer. To facilitate a low-complexity equalizer, we can approximate $\mathbf{H}_{f,N}$ with a circularly-banded matrix $\hat{\mathbf{H}}_{f,N}$, which has only non-zero power on the main diagonal, the $Q/2$ super- and sub-diagonals in a circulant sense with Q being a design parameter. Further, if we assume that the IBI $\boldsymbol{\epsilon}_{f,N}$ is small enough to be ignored and use the statistical assumptions given before, a minimum mean square error (MMSE) block equalizer[1] can be found as

$$\hat{\mathbf{s}} = \mathbf{F}_N^H\hat{\mathbf{H}}_{f,N}^H(\hat{\mathbf{H}}_{f,N}\hat{\mathbf{H}}_{f,N}^H + \mathbf{R}_{v,N})^{-1}\mathbf{y}_{f,N}, \qquad (7)$$

with $\mathbf{R}_{v,N} := \mathcal{E}\{\mathbf{v}_{f,N}\mathbf{v}_{f,N}^H\} = \sigma^2\mathbf{F}_N\mathcal{D}\{\mathbf{w}_N \odot \mathbf{w}_N^*\}\mathbf{F}_N^H$. In the above, most computational complexity is invested in inverting the covariance matrix. Assuming that the window is properly designed such that $\mathbf{R}_{v,N}$ is strictly banded with bandwidth $2Q + 1$, just like the product $\hat{\mathbf{H}}_{f,N}\hat{\mathbf{H}}_{f,N}^H$, (7) can be computed with a complexity that is linear in N and square in Q [3].

In order to improve the precision of the equalizer in (7), we need to design the window such that the IBI $\|\boldsymbol{\epsilon}_{f,N}\|^2$ as well as the band approximation error $\|\mathbf{H}_{f,N} - \hat{\mathbf{H}}_{f,N}\|^2$ will be minimized in an average sense. Besides, due to the usage of the banded MMSE block equalizer, the noise covariance $\mathbf{R}_{v,N}$ should also be banded. This will be discussed next.

---

[1] Although this paper considers only the MMSE block equalizer, other equalization schemes that exploit the circularly banded structure of the FD channel matrix are also applicable, e,g, the iterative MMSE serial equalizer in [2].

3.2. Window Design for the ODM

We first address the noise-shaping behavior of the window and rewrite the noise covariance matrix as

$$\mathbf{R}_{v,N} = \sigma^2 \underbrace{\mathbf{F}_N \mathcal{D}\{\mathbf{w}_N\}\mathbf{F}_N^H}_{\mathcal{W}_{f,N}} \underbrace{\mathbf{F}_N \mathcal{D}\{\mathbf{w}_N^*\}\mathbf{F}_N^H}_{\mathcal{W}_{f,N}^H}. \qquad (8)$$

To enforce a strictly-banded $\mathbf{R}_{v,N}$, we follow the approach given in [3], which expresses the window $\mathbf{w}_N$ as a weighted sum of $Q+1$ complex exponentials:

$$\mathbf{w}_N = \mathbf{B}_N \mathbf{d}, \qquad (9)$$

where $\mathbf{B}_N$ is comprised of the first $Q/2 + 1$ and the last $Q/2$ columns of $\mathbf{F}_N$; $\mathbf{d}$ is a $(Q+1)$-long vector containing all the weighting coefficients. It is easy to derive that

$$\mathcal{W}_{f,N} = \sum_{q=0}^{Q} [\mathbf{d}]_q \mathbf{F}_N \mathcal{D}\{\mathbf{B}_N \mathbf{e}_q\}\mathbf{F}_N^H, \qquad (10)$$

where the product $\mathbf{F}_N \mathcal{D}\{\mathbf{B}_N \mathbf{e}_q\}\mathbf{F}_N^H$ is an identity matrix but with its columns circularly shifted over $q - Q/2$ positions. Hence, $\mathcal{W}_{f,N}$ is a strictly banded matrix and so is $\mathbf{R}_{v,N}$. Structured as the weighted sum of $Q+1$ complex exponentials, the window design boils down to the design of the coefficients $\mathbf{d}$.

Under the statistical assumption given before, we understand that minimizing the IBI $\|\boldsymbol{\epsilon}_{f,N}\|^2$ that is averaged over the data symbols amounts to minimizing $\|\boldsymbol{\epsilon}_{f,N}\|^2 \sim \|\mathcal{D}\{\mathbf{w}_N\}\mathbf{H}_{i,N}\boldsymbol{\Phi}_N\|^2$, where we have explicitly taken a possible guard interval into account through a diagonal matrix

$$\boldsymbol{\Phi}_N := \mathcal{D}\{[\mathbf{1}_{1\times(L-L_z)}, \mathbf{0}_{1\times L_z}]^T\}. \qquad (11)$$

To minimize the band approximation error $\|\mathbf{H}_{f,N} - \hat{\mathbf{H}}_{f,N}\|^2$, we are aware that a strictly banded FD matrix $\hat{\mathbf{H}}_{f,N}$ corresponds in the time domain to an $N \times N$ matrix $\hat{\mathbf{H}}_N$ that is a sum of $Q+1$ circulant matrices, each weighted by a diagonal exponential matrix:

$$\hat{\mathbf{H}}_N := \sum_{q=0}^{Q} \mathcal{D}\{\mathbf{B}_N \mathbf{e}_q\}\mathbf{C}_N^q, \qquad (12)$$

where $\mathbf{C}_N^q$ is a circulant matrix whose first column is defined as $[c_{q,0}, \cdots, c_{q,L}, \mathbf{0}_{1\times(N-L-1)}]^T$ with the coefficients $c_{q,l}$ standing for some unknowns. Analogous to $\mathcal{W}_{f,N}$ in (8), the above definition suggests that $\hat{\mathbf{H}}_{f,N} = \mathbf{F}_N \hat{\mathbf{H}}_N \mathbf{F}_N^H$ can be considered as a sum of $Q+1$ matrices, where each summand denoted as $\mathbf{F}_N \mathcal{D}\{\mathbf{B}_N \mathbf{e}_q\}\mathbf{C}_N^q \mathbf{F}_N^H$ is actually a diagonal matrix, but with its columns circularly shifted over $q - Q/2$ positions. With such a link established, we can translate the band approximation error into the time

domain as $\|\mathbf{H}_{f,N} - \hat{\mathbf{H}}_{f,N}\|^2 = \|\mathcal{D}\{\mathbf{w}_N\}\mathbf{H}_N - \hat{\mathbf{H}}_N\|^2$. Since we only need to focus on the non-zero elements in $\mathcal{D}\{\mathbf{w}_N\}\mathbf{H}_N$ and $\hat{\mathbf{H}}_N$, this leads to

$$\|\mathbf{H}_{f,N} - \hat{\mathbf{H}}_{f,N}\|^2 = \|\mathcal{D}\{\mathbf{w}_N\}\mathcal{H} - \mathbf{B}_N \mathcal{C}\|^2, \qquad (13)$$

where $\mathcal{C}$ is a $(Q+1) \times (L+1)$ matrix collecting all the coefficients $[\mathcal{C}]_{q,l} = c_{q,l}$, and $\mathcal{H}$ is an $N \times (L+1)$ matrix collecting all the channel taps $[\mathcal{H}]_{n,l} = h_{n,l}$. The RHS of the above equality is reminiscent of those works that use a basis expansion model (BEM), which is $\mathbf{B}_N$ in this context, to fit the TV channel $\mathcal{D}\{\mathbf{w}_N\}\mathcal{H}$. Therefore, the band approximation error can also be interpreted as a BEM modeling error. In particular, with the entries defined as $[\mathbf{B}_N]_{p,q} = \frac{1}{\sqrt{N}} e^{-j\frac{2\pi}{N}p(q-\frac{Q}{2})}$, this BEM corresponds to a critically-sampled complex exponential BEM ((C)CE-BEM) [6], whose exponential period equals the block length N.

In summary, we come up with the following cost function

$$\underset{\mathcal{C},\mathbf{w}_N\|\|\mathbf{w}_N\|^2=N}{\arg\min}$$
$$\mathcal{E}\{\|\mathcal{D}\{\mathbf{w}_N\}\mathcal{H} - \mathbf{B}_N \mathcal{C}\|^2\} + \theta\mathcal{E}\{\|\mathcal{D}\{\mathbf{w}_N\}\mathbf{H}_{i,N}\boldsymbol{\Phi}_{zp}\|^2\}, \qquad (14)$$

where θ is a weight factor. To solve above, we first solve for $\mathcal{C}$, which leads to $\mathcal{C} = \mathbf{B}_N^\dagger \mathcal{D}\{\mathbf{w}_N\}\mathcal{H}$, and thus the problem becomes

$$\underset{\mathbf{w}_N\|\|\mathbf{w}_N\|^2=N}{\arg\min} \quad \mathrm{tr}\left(\mathcal{P}_{\mathbf{B},N}\mathcal{D}\{\mathbf{w}_N\}\mathbf{R}_H \mathcal{D}\{\mathbf{w}_N^H\}\mathcal{P}_{\mathbf{B},N}^H\right)$$
$$+ \theta\mathrm{tr}\left(\mathcal{D}\{\mathbf{w}_N\}\mathbf{R}_\epsilon \mathcal{D}\{\mathbf{w}_N^H\}\right), \qquad (15)$$

with $\mathcal{P}_{\mathbf{B},N} := \mathbf{I}_N - \mathbf{B}_N (\mathbf{B}_N^H \mathbf{B}_N)^{-1} \mathbf{B}_N^H$, $\mathbf{R}_H := \mathcal{E}\{\mathcal{H}\mathcal{H}^H\}$, and $\mathbf{R}_\epsilon := \mathcal{E}\{\mathbf{H}_{i,N}\boldsymbol{\Phi}_N \mathbf{H}_{i,N}^H\}$. Under the WSSUS channel assumption, it is easy to see that

$$[\mathbf{R}_H]_{m,n} = \sum_{l=0}^{L} \sigma_l^2 \gamma_{m-n}. \qquad (16)$$

Likewise, we can derive from (11) that $\mathbf{R}_\epsilon$ is an $N \times N$ diagonal matrix with its pth diagonal equal to $\sum_{l=p+L_z+1}^{L} \sigma_l^2$ if $p < L - L_z$, or zero otherwise. Substituting (9) in (15) leads further to

$$\underset{\mathbf{d}\|\|\mathbf{d}\|^2=N}{\arg\min} \ \mathbf{d}^T \boldsymbol{\mathcal{X}}_N \mathbf{d}^*, \qquad (17)$$

with $\boldsymbol{\mathcal{X}}_N := \mathbf{B}_N^T \left(\sum_{n=0}^{N-1} \mathcal{D}\{\mathbf{e}_n^T \mathcal{P}_{\mathbf{B},N}\}\mathbf{R}_H \mathcal{D}\{\mathcal{P}_{\mathbf{B},N}^H \mathbf{e}_n\} + \theta\mathbf{R}_\epsilon\right)\mathbf{B}_N^*$. Hence, $\mathbf{d}$ is the eigenvector corresponding to the least significant eigenvalue of $\boldsymbol{\mathcal{X}}_N^*$.

A similar windowing strategy is also presented in [2], which maximizes the signal to interference and noise ratio (SINR) directly in the frequency domain. The difference is that this paper translates the interference coming from the band

approximation error into the (C)CE-BEM modeling error. Actually, it can be shown that in the absence of noise and IBI, and assuming the window is as long as the observation sample block, the window of [2] will admit the same expression as the ODM window. Indeed, as we will observe in the simulation part, the performances of these two approaches are very close to each other.

¿From the above, it is not difficult to understand that a weakness of the ODM window, and hence that of [2] as well, is associated with the relatively large BEM modeling error. This is typical to the (C)CE-BEM, which in general is not very good at fitting a realistic TV channel as demonstrated in [8]. The same paper shows that the (O)CE-BEM [7], which is equipped with a larger exponential period, can improve the BEM modeling performance considerably. This idea will be explored in the next section.

4. FD EQUALIZATION BASED ON THE EDM

4.1. Equalization Scheme

For reasons that will become clear later on, we extend the data model in (3) by appending $K - N$ zeros to the end of $\mathbf{y}_N$ with $K \geq N + L$, and thereby coin a virtual data model of a larger scale:

$$\underbrace{\begin{bmatrix} \mathbf{y}_N \\ \mathbf{0}_{(K-N)\times 1} \end{bmatrix}}_{\mathbf{y}_K} = \underbrace{\begin{bmatrix} \mathcal{D}\{\mathbf{w}_N\}\bar{\mathbf{H}}_K & \mathcal{D}\{\mathbf{w}_N\}\mathbf{H}_{i,K} \\ \mathbf{X} & \mathbf{U} \end{bmatrix}}_{\mathbf{H}_K} \underbrace{\begin{bmatrix} \mathbf{s} \\ \mathbf{a} \end{bmatrix}}_{\mathbf{s}_K}$$
$$+ \underbrace{\begin{bmatrix} \mathcal{D}\{\mathbf{w}_N\}\mathbf{H}_{i,K} \\ \mathbf{0}_{(K-N)\times(K-N)} \end{bmatrix} \left(\begin{bmatrix} \mathbf{0}_{(K-N-L)\times 1} \\ \mathbf{s}_{\text{pre}} \end{bmatrix} - \mathbf{a} \right)}_{\boldsymbol{\epsilon}_K} + \underbrace{\begin{bmatrix} \mathbf{v} \\ \mathbf{0}_{(K-N)\times 1} \end{bmatrix}}_{\mathbf{v}_K},$$

(18)

where $\bar{\mathbf{H}}_K$ is an $N \times N$ matrix with entries $[\bar{\mathbf{H}}_K]_{p,n} := h_{p,p-n}$; $\mathbf{H}_{i,K}$ is an $N \times (K - N)$ matrix with entries $[\mathbf{H}_{i,K}]_{p,n} := h_{p,p-n+K-N}$; $\mathbf{X}$ is a $(K - N) \times N$ matrix with entries $[\mathbf{X}]_{p,n} := \tilde{h}_{p,p-n+N}$, and $\mathbf{U}$ is a $(K - N) \times (K - N)$ matrix with entries $[\mathbf{U}]_{p,n} := \tilde{h}_{p,p-n}$. The coefficients $\tilde{h}_{p,l}$ in $\mathbf{X}$ and $\mathbf{U}$ stand for virtual channel taps, which are assumed to be zero if $l < 0$ or $l > L$. The EDM in the absence of noise is illustrated in Fig. 2. Obviously, to guarantee the validity of (18), especially the introduced extra zeros in $\mathbf{y}_K$, we require $\mathbf{Xs} + \mathbf{Ua} = \mathbf{0}$. Since the first $N - L$ columns of $\mathbf{X}$ are all zeros, this means

$$\mathbf{a} = -\mathbf{U}^{-1}\mathbf{X}\mathbf{Z}_{N-L}\mathbf{s}_{\text{post}}, \tag{19}$$

with $\mathbf{Z}_{N-L} := [\mathbf{0}_{L\times(N-L)}, \mathbf{I}_L]^T$.

It is straightforward to see that $\boldsymbol{\epsilon}_K$, the second term on the RHS of (18) is due to the IBI, whose first N elements,

with (19) taken into account, can be expressed as

$$\mathcal{D}\{\mathbf{w}_N\}\mathbf{H}_{i,K}\left(\begin{bmatrix} \mathbf{0}_{(K-N-L)\times 1} \\ \mathbf{s}_{\text{pre}} \end{bmatrix} + \mathbf{U}^{-1}\mathbf{X}\mathbf{Z}_{N-L}\mathbf{s}_{\text{post}} \right),$$

(20)

which can only be eliminated by the ZP.

Transformed into the frequency domain, the EDM in (18) becomes:

$$\mathbf{y}_{f,K} = \mathbf{H}_{f,K}\mathbf{F}_K\mathbf{s}_K + \boldsymbol{\epsilon}_{f,K} + \mathbf{v}_{f,K}, \tag{21}$$

where $\mathbf{y}_{f,K} := \mathbf{F}_K\mathbf{y}_K$, and $\boldsymbol{\epsilon}_{f,K}$ and $\mathbf{v}_{f,K}$ are similarly defined as $\mathbf{y}_{f,K}$. $\mathbf{H}_{f,K}$ stands for the FD channel matrix $\mathbf{H}_{f,K} := \mathbf{F}_K\mathbf{H}_K\mathbf{F}_K^H$, which is in principle a full matrix. Like in the previous section, we use a strictly banded matrix $\hat{\mathbf{H}}_{f,K}$ to approximate $\mathbf{H}_{f,K}$ with $\hat{\mathbf{H}}_{f,K}$ having nonzero entries only on the main diagonal, the $Q/2$ super- and the $Q/2$ sub-diagonals. Besides, we assume that the IBI $\boldsymbol{\epsilon}_{f,K}$ can be neglected and $\mathcal{E}\{\mathbf{s}_K\mathbf{s}_K^H\} \approx \mathbf{I}_K$. The resulting MMSE block equalizer can thus be expressed as

$$\hat{\mathbf{s}} = \mathbf{Z}_{K-N}^H\mathbf{F}_K^H\hat{\mathbf{H}}_{f,K}^H(\hat{\mathbf{H}}_{f,K}\hat{\mathbf{H}}_{f,K}^H + \mathbf{R}_{v,K})^{-1}\mathbf{y}_{f,K}, \tag{22}$$

with

$$\mathbf{Z}_{K-N} := [\mathbf{I}_N, \mathbf{0}_{N\times(K-N)}]^T,$$
$$\mathbf{R}_{v,K} := \sigma^2\mathbf{F}_K\mathbf{Z}_{K-N}(\mathbf{w}_N \odot \mathbf{w}_N^*)^T\mathbf{Z}_{K-N}^H\mathbf{F}_K^H.$$

It can be imagined that to enhance the equalization performance, the window in the EDM assumes a three-fold task: 1) to make the noise covariance matrix $\mathbf{R}_{v,K}$ strictly banded; 2) to minimize the IBI $\|\boldsymbol{\epsilon}_{f,K}\|^2$; and 3) to minimize the band approximation error $\|\mathbf{H}_{f,K} - \hat{\mathbf{H}}_{f,K}\|^2$.
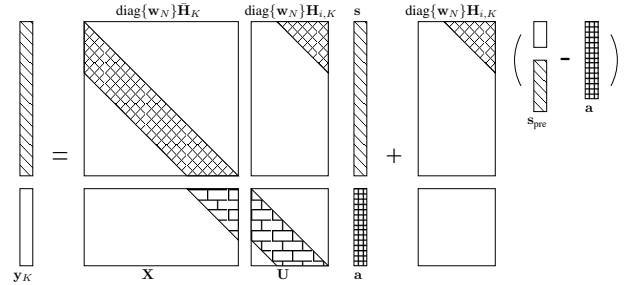

Figure 2: The noiseless extended data model.

4.2. Window Design for the EDM

Let us first address the noise-shaping behavior of the window. Unfortunately, it is impossible for $\mathbf{R}_{v,K}$ to be strictly banded [11]. As a compromise, we relax the requirement by approximating

$$\mathbf{R}_{v,K} \approx \sigma^2\mathbf{F}_K\mathcal{D}\{\mathbf{w}_K \odot \mathbf{w}_K^*\}\mathbf{F}_K^H, \tag{23}$$

where $\mathbf{w}_K := [\mathbf{w}_N^T, \mathbf{w}_{K-N}^T]^T$ with $\mathbf{w}_{K-N}$ being a non-zero vector of length $K - N$, whose components are subject to the window design. Analogous to the previous section, we set $\mathbf{w}_K = \mathbf{B}_K \mathbf{d}$ with $\mathbf{B}_K$ standing for a $K \times (Q+1)$ matrix, which is comprised of the first $Q/2+1$ and the last $Q/2$ columns of $\mathbf{F}_K$. Consequently, the window for the EDM admits the expression

$$\mathbf{w}_N = \bar{\mathbf{B}}_K \mathbf{d}, \qquad (24)$$

where $\bar{\mathbf{B}}_K$ consists of the first N rows of $\mathbf{B}_K$.

¿From (20), we understand that to suppress the IBI $\|\boldsymbol{\epsilon}_{f,K}\|^2$, it is sufficient to minimize $\|\mathcal{D}\{\mathbf{w}_N\}\mathbf{H}_{i,K}\boldsymbol{\Phi}_K\|^2$, where we have introduced the matrix

$$\boldsymbol{\Phi}_K := \mathcal{D}\{[\mathbf{0}_{1\times(K-N-L)}, \mathbf{1}_{1\times(L-L_z)}, \mathbf{0}_{1\times L_z}]^T\}, \quad (25)$$

which takes a possible ZP into account.

To minimize the difference $\|\mathbf{H}_{f,K} - \hat{\mathbf{H}}_{f,K}\|^2$, we go back again to the time domain and consider the matrix [c.f. (12)]

$$\hat{\mathbf{H}}_K = \sum_q \mathcal{D}\{\mathbf{B}_K \mathbf{e}_q\}\mathbf{C}_K^q, \qquad (26)$$

where $\mathbf{C}_K^q$ is a circulant matrix with its first column defined as $[c_{q,0}, \cdots, c_{q,L}, \mathbf{0}_{1\times(K-L-1)}]^T$. Regarding $\hat{\mathbf{H}}_K$ as the time-domain counterpart of the strictly banded $\hat{\mathbf{H}}_{f,K}$, we can readily establish the link $\|\mathbf{H}_{f,K} - \hat{\mathbf{H}}_{f,K}\|^2 = \|\mathbf{H}_K - \hat{\mathbf{H}}_K\|^2$. Recalling that in (18) the virtual channel tap $\tilde{h}_{p,n}$ contained in $\mathbf{X}$ and $\mathbf{U}$ is subject to design, we can simply let $\tilde{h}_{p,n} = \frac{1}{\sqrt{K}}\sum_{q=0}^Q e^{-j\frac{2\pi}{K}(p+N)(q-\frac{Q}{2})}c_{q,n}$. In this way, the non-zero elements of $\mathbf{H}_K$ and $\hat{\mathbf{H}}_K$ will differ only in the first N rows. Borrowing the notations $\mathcal{H}$ and $\mathcal{C}$ defined in (13), we can express the approximation error as $\|\mathbf{H}_{f,K} - \hat{\mathbf{H}}_{f,K}\|^2 = \|\mathcal{D}\{\mathbf{w}_N\}\mathcal{H} - \bar{\mathbf{B}}_K\mathcal{C}\|^2$. With entries $[\bar{\mathbf{B}}_K]_{p,q} = \frac{1}{\sqrt{K}}e^{-j\frac{2\pi}{K}p(q-\frac{2}{Q})}$, the $N \times (Q+1)$ matrix $\bar{\mathbf{B}}_K$ tallies with the definition of an (O)CE-BEM [7], which has an exponential period K that is larger than the block size N.

Finally, we come up with the cost function for the EDM case

$$\begin{array}{c}\arg\min\\ \mathcal{C},\mathbf{w}_N|\|\mathbf{w}_N\|^2=N\end{array}$$
$$\mathcal{E}\{\|\mathcal{D}\{\mathbf{w}_N\}\mathcal{H} - \bar{\mathbf{B}}_K\mathcal{C}\|^2\} + \theta\mathcal{E}\{\|\mathcal{D}\{\mathbf{w}_N\}\mathbf{H}_{i,K}\boldsymbol{\Phi}_K\|^2\}. \qquad (27)$$

Following the same steps as in the previous section, we can find the window coefficients $\mathbf{d}$ as the eigenvector corresponding to the least significant eigenvalue of $\boldsymbol{\mathcal{X}}_K^*$ with

$$\boldsymbol{\mathcal{X}}_K := \bar{\mathbf{B}}_K^T\Big(\sum_{n=0}^{N-1}\mathcal{D}\{\mathbf{e}_n^T\boldsymbol{\mathcal{P}}_{\bar{\mathbf{B}},K}\}\mathbf{R}_H\mathcal{D}\{\boldsymbol{\mathcal{P}}_{\bar{\mathbf{B}},K}^H\mathbf{e}_n\} + \theta\mathbf{R}_\epsilon\Big)\bar{\mathbf{B}}_K^*,$$

$$\boldsymbol{\mathcal{P}}_{\bar{\mathbf{B}},K} := \mathbf{I}_N - \bar{\mathbf{B}}_K(\bar{\mathbf{B}}_K^H\bar{\mathbf{B}}_K)^{-1}\bar{\mathbf{B}}_K^H.$$
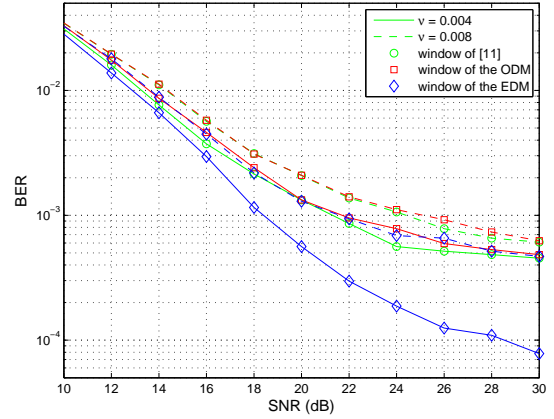

Figure 3: BER performance.

5. NUMERICAL RESULTS

We test the proposed algorithms over Jakes' channels [12] with $L + 1 = 31$ channel taps. The variance of the lth tap is $\sigma_l^2 = e^{-\frac{l}{10}}$, and the normalized time correlation is $\gamma_m = J_0(2\pi\nu m)$, where $J_0(\cdot)$ denotes the zeroth-order Bessel function of the first kind, and ν for the normalized Doppler spread, which is chosen to be $\nu = 0.004$.

To obtain the ODM and EDM window, we use $\theta = 0.4$ in the cost functions. Besides, we set $[N, Q] = [256, 2]$ for the ODM window as well as for the window of [2], and $[N, K, Q] = [128, 256, 2]$ for the EDM window. In this way, the MMSE block equalizer will have the same complexity for all three schemes. QPSK modulated symbols are transmitted and we compare the bit error rate (BER) only on the 32 data symbols that lie in the middle of the block, i.e., we assume a sliding window approach [2]. This is to mitigate the absence of the ZP, i.e., $L_z = 0$. From Fig. 3, we can observe that the ODM window has a similar performance as the window of [2], both of which suffer a higher noise floor than the EDM window.

6. REFERENCES

[1] D. Falconer, S. L. Ariyavisitakul, A. Benyamin-Seeyar, and B. Eidson, "Frequency domain equalization for single-carrier broadband wireless systems," *IEEE Communications Magazine*, vol. 40, no. 9, pp. 58–66, Apr. 2002.

[2] P. Schniter and H. Liu, "Iterative frequency-domain equalization for single-carrier systems in doubly-dispersive channels," *Asilomar Conference on Signals, Systems, and Computers*, pp. 667–671, Nov 2004.

[3] L. Rugini, P. Banelli, and G. Leus, "Low-complexity banded equalizers for OFDM systems in Doppler spread channels," *EURASIP Journal on Applied Signal Processing*, vol. 2006, pp. Article ID 67404, 13 pages, 2006.

[4] P. Schniter, "Low-complexity equalization of OFDM in doubly-selective channels," *IEEE Transactions on Signal Processing*, vol. 52, no. 4, pp. 1002–1011, Apr 2004.

[5] M. K. Tsatsanis and G. B. Giannakis, "Modeling and equalization of rapidly fading channels," *International Journal of Adaptive Control and Signal Processing*, vol. 10, no. 2/3, pp. 159–176, Mar. 1996.

[6] G. B. Giannakis and C. Tepedelenlioğlu, "Basis expansion models and diversity techniques for blind identification and equalization of time-varying channels," *Proceedings of the IEEE*, vol. 86, no. 10, pp. 1969–1986, Oct. 1998.

[7] T. A. Thomas and F. W. Vook, "Multi-user frequency-domain channel identification, interference suppression, and equalization for time-varying broadband wireless communications," *Proceedings of the 2000 IEEE Sensor Array and Multichannel Signal Processing Workshop*, pp. 444–448, Mar. 2000.

[8] T. Zemen and C. F. Mecklenbräuker, "Time-variant channel estimation using discrete prolate spheroidal sequences," *IEEE Transactions on Signal Processing*, vol. 53, no. 9, pp. 3597– 3607, Sept. 2005.

[9] Z. Wang, X. Ma, and G. B. Giannakis, "OFDM or single-carrier block transmissions?," *IEEE Transactions on Communications*, vol. 52, no. 3, pp. 380–394, Mar. 2004.

[10] L. Deneire, B. Gyselinckx, and M. Engels, "Training sequence versus cyclic prefix - a new look on single carrier communication," *IEEE Communications Letters*, vol. 7, no. 5, pp. 292–294, 2001.

[11] Z. Tang and G. Leus, "Receiver design for single-carrier transmission over time-varying channels," *International Conference on Acoustics, Speech, and Signal Processing, ICASSP*, 2007.

[12] W. C. Jakes, *Microwave Mobile Channels*, New York: Wiley, 1974.